RNA (1996), 2:674–681. Cambridge University Press. Printed in the USA.

Differences in the interaction of *Escherichia coli* RNase P RNA with tRNAs containing a short or a long extra arm

RAJESH K. GAUR,[1] ANDREAS HANNE, FRANK CONRAD, DIETMAR KAHLE, and GUIDO KRUPP
Institut für Allgemeine Mikrobiologie, Christian-Albrechts-Universität, Am Botanischen Garten 9, D-24118 Kiel, Germany

ABSTRACT

The phosphorothioate footprinting technique was applied to the investigation of phosphate moieties in tRNA substrates involved in interactions with M1 RNA, the catalytic subunit of *Escherichia coli* RNase P. In general agreement with previous data, all affected sites were localized in acceptor stem and T arm. But the analyzed examples for class I (*Saccharomyces cerevisiae* pre-tRNA^{Phe} with short variable arm) and class II tRNAs (*E. coli* pre-tRNA^{Tyr} with large variable arm) revealed substantial differences. In the complex with pre-tRNA^{Phe}, protection was observed at U55, C56, and G57, along the top of the T loop in the tertiary structure, whereas in pre-tRNA^{Tyr}, the protected positions were G57, A58, and A59, at the bottom of the T loop. These differences suggest that the size of the variable arm affects the spatial arrangement of the T arm, providing a possible explanation for the discrepancy in reports about the D arm requirement in truncated tRNA substrates for eukaryotic RNase P enzymes. Enhanced reactivities were found near the junction of acceptor and T stem (U6, 7, 8 in pre-tRNA^{Phe} and G7, U63, U64 in pre-tRNA^{Tyr}). This indicates a partial unfolding of the tRNA structure upon complex formation with RNase P RNA.

Keywords: footprinting; phosphorothioates; substrate recognition; tRNA^{Phe}; tRNA processing; tRNA^{Tyr}

INTRODUCTION

RNase P is required for the processing of pre-tRNAs and generates the 5′-termini of mature tRNAs by an endonucleolytic removal of the 5′-flank. The isolated RNA subunit of eubacterial RNase P can perform this highly specific reaction with a strict requirement of divalent cations (Altman et al., 1993). Binding of RNase P to the pre-tRNA involves specific regions of both reactants, substrate and enzyme. The interaction between pre-tRNA substrate and RNase P has been studied with several approaches, including UV crosslinking (Guerrier-Takada et al., 1989; Burgin & Pace, 1990), introduction of modifications in the exocyclic bases (Kahle et al., 1990; Thurlow et al., 1991), the phosphate backbone (Gaur & Krupp, 1993; Conrad et al., 1995), and the 2′-hydroxyl groups (Perreault & Altman, 1992; Gaur & Krupp, 1993; Kleineidam et al., 1993; Smith & Pace, 1993; Conrad et al., 1995). The changed accessibility of bases to chemical modifications in the complex between *Escherichia coli* RNase P RNA (M1 RNA) and pre-tRNA was used for footprinting studies (Knap et al., 1990). Recently, phosphorothioates were used for detailed footprinting studies of tRNA complexes with cognate synthetases (Schatz et al., 1991; Rudinger et al., 1992). We have applied this technique to study the interaction between pre-tRNA substrates and *E. coli* RNase P RNA.

RESULTS

The S_P diastereomers of NTPs[αS] are substrates for T7 RNA polymerase and incorporated with an inversion of configuration, resulting in R_P diastereomers in the transcripts. Because unmodified NTP and NTPαS are incorporated with similar efficiency, the mixture with 95% unmodified NTP yields products with approximately one phosphorothioate position per RNA molecule (Conrad et al., 1995). In preliminary experi-

Reprint requests to: Guido Krupp, Institut für Hämatopathologie, Christian-Albrechts-Universität, Niemannsweg 11, D-24105 Kiel, Germany.
[1] Present address: Howard Hughes Medical Institute, University of Massachusetts, Medical Center, 373 Plantation Street, Worcester, Massachusetts 01605, USA.

ments, the complex formation between tRNA and RNase P RNA was monitored by a gel retardation assay (Hardt et al., 1993a) on 5% nondenaturing polyacrylamide gels with subsequent densitometer scanning of the corresponding autoradiograms; data with pre-tRNA^{Tyr} are shown in Figure 1. No significant changes in the K_d value (about 100 nM) were observed with phosphorothioate-modified tRNA^{Tyr} and tRNA^{Phe}.

The interaction of tRNA transcripts with M1 RNA was analyzed by footprinting under native conditions, this means RNase P RNA cleavage conditions with 100 mM Mg^{2+}. A renaturation step of the tRNA preceded the addition of M1 RNA, which was followed by the iodine cleavage step. We used a 50-fold molar excess of M1 RNA and, under these conditions, about 70% of the tRNA was present in the complex. It was expected that bound pre-tRNAs were cleaved by M1 RNA and a corresponding amount of 5′-matured tRNA^{Tyr} was observed (Figs. 3, 4). Comparisons of the iodine cleavage patterns of tRNAs in the presence and absence of M1 RNA revealed changed reactivities of certain phosphorothioate positions, evident by the decreased or increased band intensities in the resulting autoradiogram. The two scans were superimposed in such a fashion to minimize the number of bands with changed intensities. These adjustments were done for complete scans, whereas zoomed sections are shown in Figures 2, 3, 4, and 5. Footprint effects should persist at different iodine concentrations, and consistent data were observed at 1 mM and 3 mM iodine, similar to previous reports (Schatz et al., 1991; Rudinger et al., 1992).

Pre-tRNA^{Tyr} from *E. coli* is the best studied RNase P substrate and it was chosen as an example for a class II tRNA with a long variable arm that includes a base paired stem. In the complex with M1 RNA, protected phosphates were found at four positions: U3 near the cleavage site in the acceptor stem; G57, A58, and A59 in the middle and at the bottom of the T loop in the tertiary structure. In contrast, phosphorothioates near the junction of acceptor and T stems (G7 and U63, U64), at the top of the T loop (U54), and at the 3′-terminal CCA (C75) were more accessible to iodine in the presence of M1 RNA (Figs. 2, 3, 4). The data are summarized and presented in the cloverleaf sequence (Fig. 6) and in a tertiary structure model (Fig. 7).

For *Saccharomyces cerevisiae* tRNA^{Phe}, a class I tRNA with short extra arm, a wealth of detailed structural data is available (Quigley & Rich, 1976). Here, protected phosphates were found at six positions: U55, C56, and G57 at the top and in the middle of the T loop in the tertiary structure; in addition, G71 and C72, juxtaposed to the cleavage site in the acceptor stem, and also C75 at the CCA-end. Similar to pre-tRNA^{Tyr}, exposed phosphorothioates were found near the junction of acceptor and T stems (U6, 7, 8). An example is shown in Figure 5 and data are presented in cloverleaf form (Fig. 6) and in a tertiary structure model (Fig. 7).

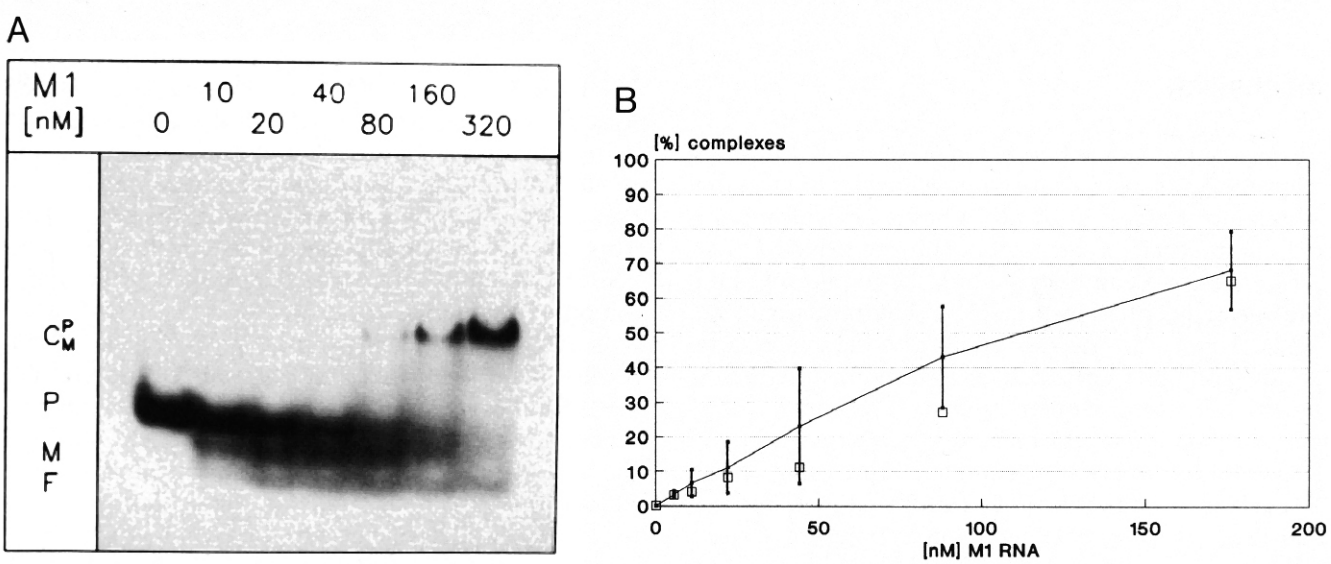

FIGURE 1. Gel retardation assays. **A:** Autoradiogram with phosphorothioate-modified *E. coli* pre-tRNA^{Tyr}, containing 5% GTPαS and internally labeled with [α-^{32}P]-UTP. pre-tRNA (10 nM) was incubated with the indicated concentrations of M1 RNA. The positions of the complex with M1 RNA (C^P_M; complexes with pre-tRNA and 5′-matured tRNA comigrate), free pre-tRNA (P), free 5′-matured tRNA (M), and the free 5′-flank (F) are marked. **B:** Binding curves. The fraction of the complexes with M1 RNA were determined from densitometer tracings of autoradiograms as shown in A, performing three independent experiments for each transcript. In A, the concentrations of total M1 RNA are indicated, whereas here the values refer to "active M1 RNA," meaning 55% of the total M1 RNA (Hardt et al., 1993a). Small black squares and curve, mean values and standard deviations obtained with unmodified RNA; open squares, mean values with phosphorothioate-modified RNA (GTPαS).

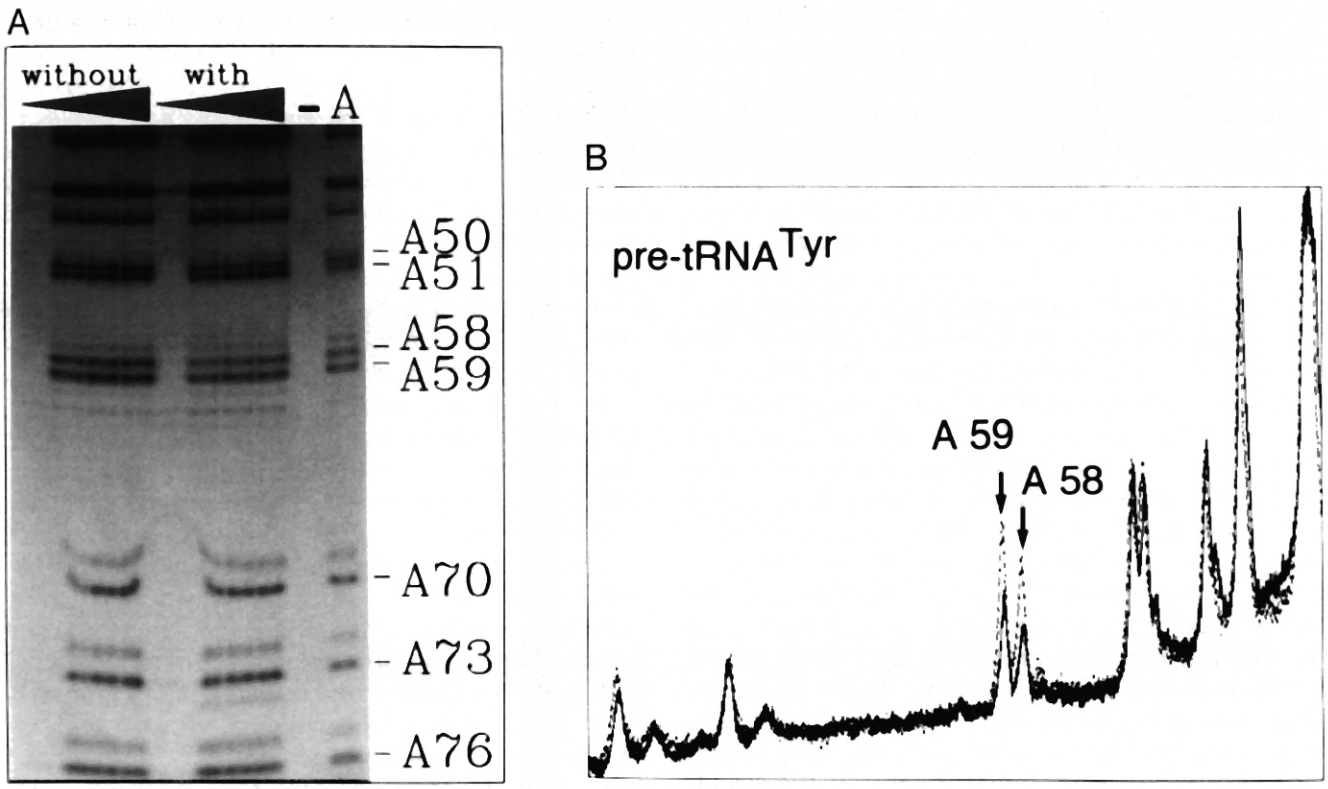

FIGURE 2. Footprint analysis of *E. coli* tRNA^{Tyr} with ATPαS. **A:** Samples were incubated under native conditions, in the absence of M1 RNA (indicated by "without") or with a 50-fold molar excess of M1 RNA ("with"). Only the section is shown where effects have been observed. From left to right, increasing concentrations of iodine were used (indicated by the wedge): 0, 0.1, 1, and 3 mM. To obtain a sequence ladder, tRNA was incubated under denaturing conditions, without (lane –) or with 3 mM iodine (lane A). Bands were assigned to adenosines in the tRNA sequence. **B:** Densitometer curves to compare the lanes with free tRNA (dashed line) and in the presence of M1 RNA (solid line). Bands for A58 and A59 are weaker in the complex and they are marked.

DISCUSSION

Studies of the interaction between RNase P RNA and its pre-tRNA substrate are complicated by the fact that a high molar excess of M1 RNA has to be used and this results in efficient cleavage of the pre-tRNA. Otherwise, modified conditions would be required to limit the reactivity of RNase P RNA (LaGrandeur et al., 1994). Mature tRNA was reported to behave as competitive inhibitor in the cleavage reaction of pre-tRNAs by M1 RNA with similar values for K_i and K_m, suggesting that similar characteristics govern binding of RNase P RNA to pre-tRNA and to mature tRNA (Reich et al., 1988; Smith et al., 1992; Hardt et al., 1993a, 1995; Tallsjö & Kirsebom, 1993), and contact points in RNase P RNA have been identified by crosslinking with mature tRNA^{Phe} (Burgin & Pace, 1990). But other data suggest that binding modes for pre-tRNA and mature tRNA are not identical (Guerrier-Takada & Altman, 1993; LaGrandeur et al., 1994; Westhof & Altman, 1994; see also below).

In our footprinting experiments, we combined pre-tRNA and RNase P RNA and a complex of RNase P RNA and 5′-matured tRNA was formed and analyzed for affected sites in the mature tRNA domains. Footprinting requires low levels of phosphorothioates in the tRNA transcripts, and it was important to know if this affected complex formation with RNase P RNA. This was not the case, because the K_d values of about 100 nM were unchanged, as determined by gel retardation experiments.

In different studies (Guerrier-Takada et al., 1989; Kahle et al., 1990; Knap et al., 1990; Thurlow et al., 1991; Gaur & Krupp, 1993; Conrad et al., 1995), important contact regions in the pre-tRNA were localized in the (elongated) acceptor stem and T arm. Nevertheless, the information about bona fide contact points in pre-tRNAs was still scarce due to the limitations of these methods. Modification interference (Kahle et al., 1990; Thurlow et al., 1991; Gaur & Krupp, 1993; Conrad et al., 1995) did not differentiate between changes in pre-tRNA conformation, in substrate binding or product release, and in the rate of the cleavage step. UV crosslinking (Guerrier-Takada et al., 1989) was limited to those interacting bases with proper stereochemistry. The further analysis of the crosslinked complex for

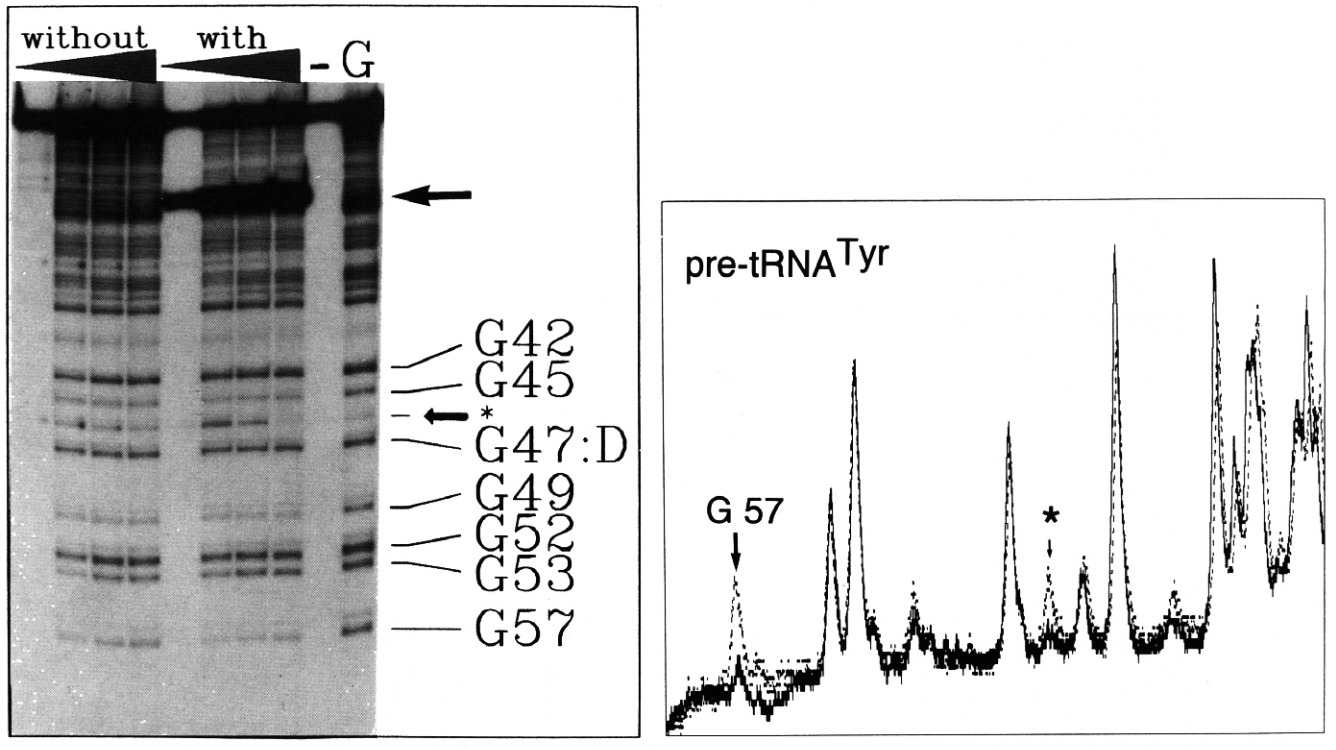

FIGURE 3. Footprint analysis of *E. coli* tRNA^{Tyr} with GTPαS. Analysis was performed as described in Figure 2. The weaker band for G57 is marked. Arrow and asterisk indicate a nonspecific background cleavage product. Pre-tRNA^{Tyr} was cleaved in the presence of M1 RNA and the position of 5′-matured tRNA is indicated by an arrow at the right margin.

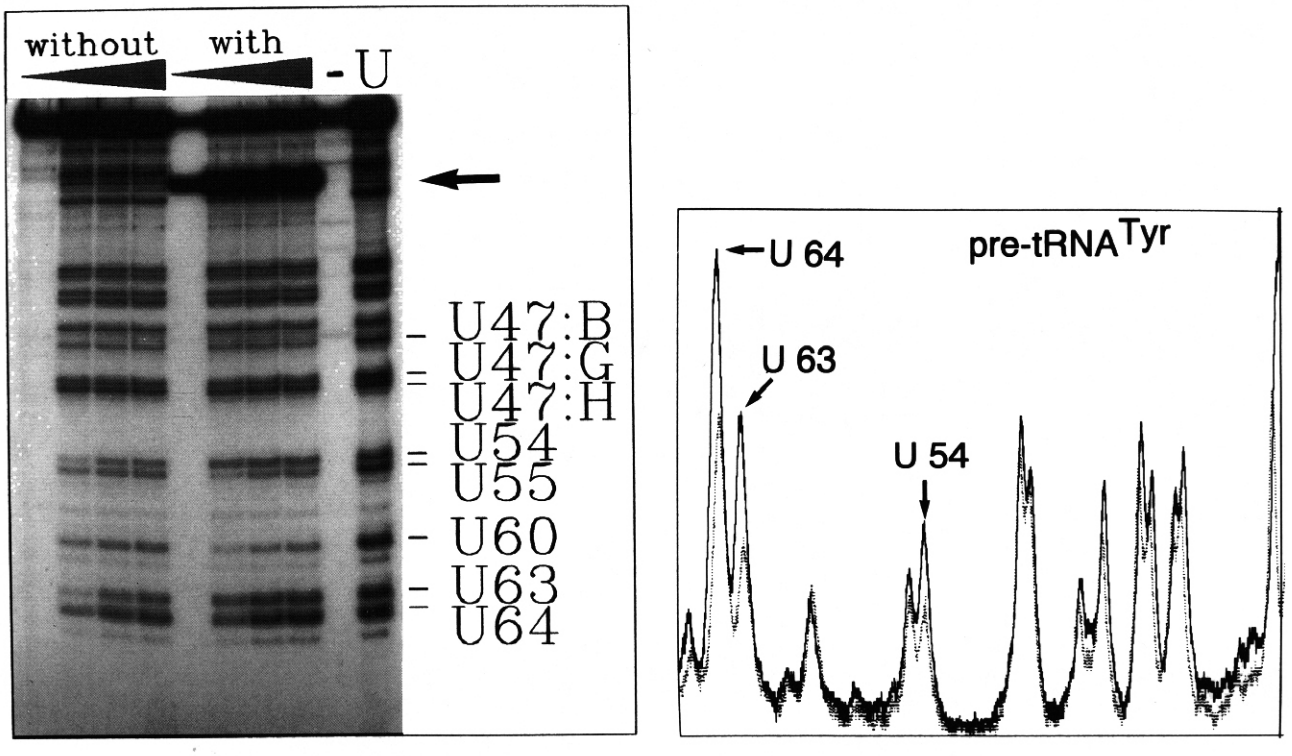

FIGURE 4. Footprint analysis of *E. coli* tRNA^{Tyr} with UTPαS. Analysis as described in Figures 2 and 3. The stronger bands in the the presence of M1 RNA are marked: U64, U63, and U54.

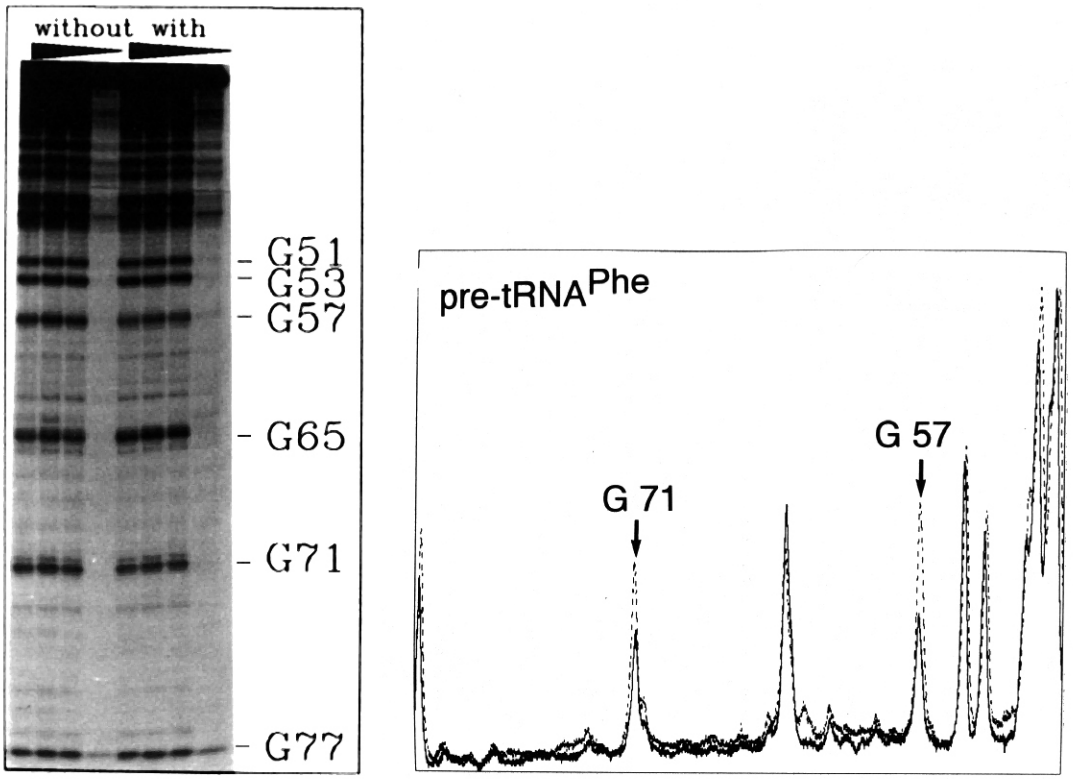

FIGURE 5. Footprint analysis of *S. cerevisiae* $tRNA^{Phe}$ with GTPαS, as described in Figure 2. The weaker bands for G71 and G57 are marked.

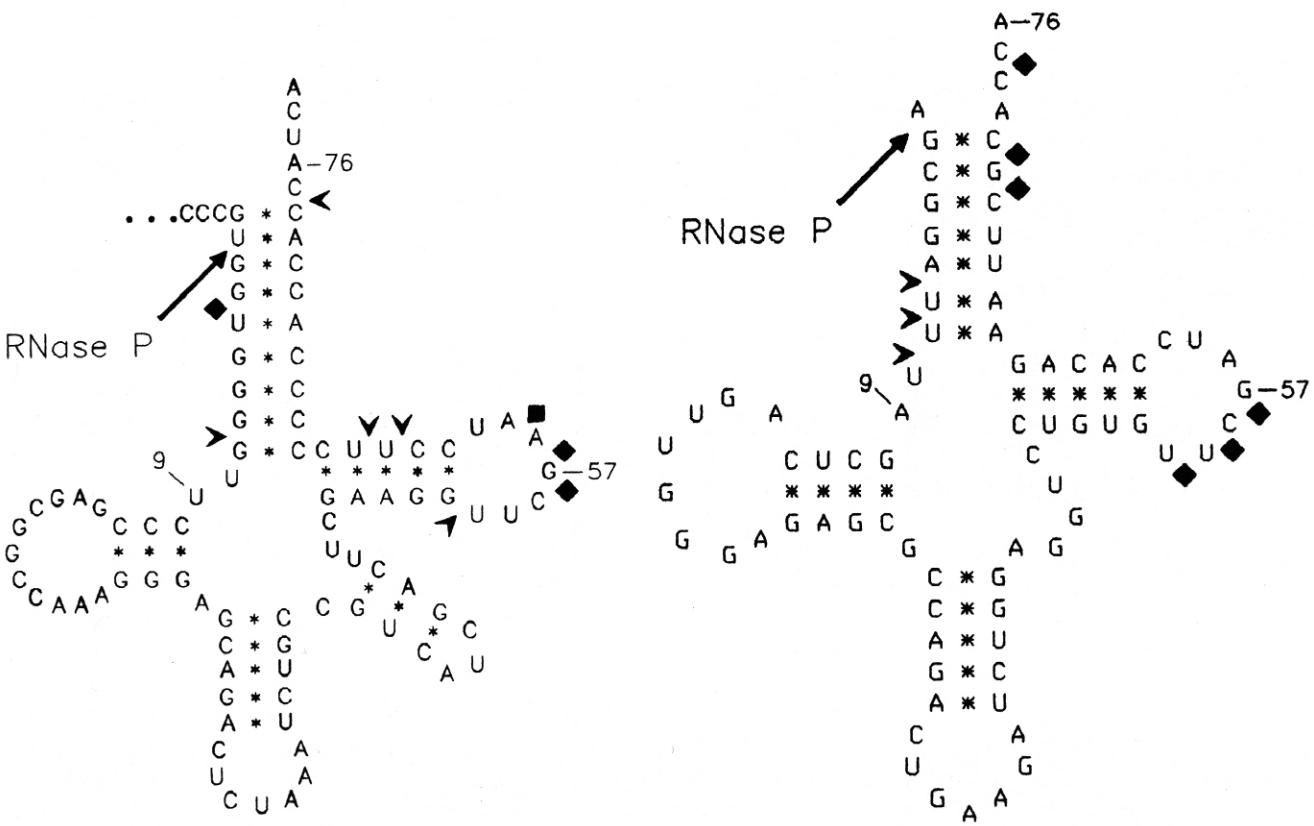

FIGURE 6. Footprint results are shown with the cloverleaf sequences of pre-$tRNA^{Tyr}$ (left) and pre-$tRNA^{Phe}$ (right). RNase P cleavage site and a short section of the 5′-flank are indicated. Protected phosphodiester positions are marked by black squares, exposed sites by arrowheads.

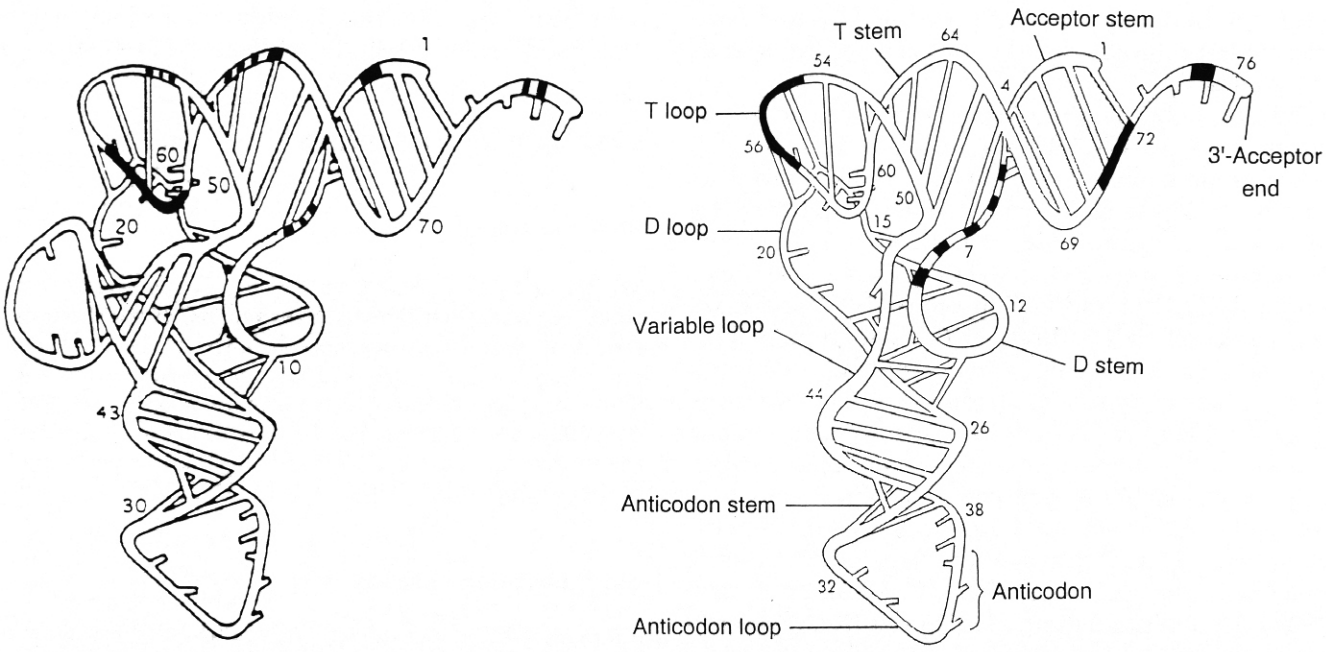

FIGURE 7. Footprint results are shown in tertiary structure models of pre-tRNA^{Tyr} (left) and pre-tRNA^{Phe} (right). Protected sites and exposed sites are represented by solid and striped bars, respectively.

changed accessibilities of bases to chemical modifications (Knap et al., 1990) did not allow a high resolution, but it was concluded that the pre-tRNA structure is partially unfolded upon complex formation. Thus, more detailed data were expected from footprints with phosphorothioate-modified RNAs, because they had allowed the very precise identification of interacting loci in complexes of tRNAs with their cognate synthetases, providing also insight into conformational changes (Schatz et al., 1991; Rudinger et al., 1992). This technique was applied to study the interactions between *E. coli* RNase P RNA (M1 RNA) and a class II tRNA with long variable arm, *E. coli* tRNA^{Tyr}, and a class I tRNA with short variable arm, *S. cerevisiae* pre-tRNA^{Phe}.

Based on modification interference analyses, possible contact points in pre-tRNAs were localized in the acceptor and T arms at the top of the L-shaped tertiary structure. This general conclusion was supported by our footprinting analysis (Figs. 6, 7). In principle, modification interference can be caused by disrupting direct contacts, but also indirectly by disturbing the tRNA tertiary structure. A comparison with footprinting data might reveal these indirect effects. Indeed, one example was found with the phosphorothioate at U9 in *E. coli* pre-tRNA^{Tyr} and A9 in yeast pre-tRNA^{Phe}. They interfered severely with RNase P cleavage (Gaur & Krupp, 1993; Conrad et al., 1995), but no effects were detected in the footprint. An explanation is provided by the low affinity of phosphorothioates to Mg^{2+} (Eckstein, 1985). The phosphate oxygens of nt 8, 9, 11, and 12 form an Mg-binding pocket (Quigley et al., 1978), which is lost upon phosphorothioate modification, thus resulting in a destabilized (or altered) tRNA tertiary structure.

The opposite effects were observed with the protected G71, C72 in pre-tRNA^{Phe}. No modification interference had been observed in this region (Kahle et al., 1990; Thurlow et al., 1991; Gaur & Krupp, 1993; Conrad et al., 1995). Furthermore, kinetic data for M1 RNA cleavage of pre-tRNA mutants with 3′ deletions in the acceptor stem revealed that only the removal of the 3′-terminal CCA sequence resulted in a sixfold increased K_m value, whereas more deletions in the 3′ half of the acceptor stem, including nt 71 and 72 (the protected sites in the footprint), had no additional effects (Svärd & Kirsebom, 1992). Without doubt, a direct interaction must occur next to the cleavage site at the 5′ end of acceptor stem. Very likely, the protected phosphates near the 3′ end are caused by indirect conformational effects, but not by direct contacts.

Although other previously identified interfering nucleotide positions coincide with footprint effects, complex formation can result in protected as well as in more accessible phosphate groups, depending on the local structure. For example, direct interaction of RNase P RNA with the 3′-terminal CCA was demonstrated clearly (Harris et al., 1994; Kirsebom & Svärd, 1994; Westhof & Altman, 1994), but different effects were observed with the two tRNAs. The free CCA end in pre-tRNA^{Phe} is flexible and complex formation with M1 RNA resulted in a protected phosphate at C75. How-

ever, the flexibility is reduced by the extended base pairing in pre-tRNA^{Tyr} and C75 was more exposed in the complex.

Interestingly, modification interference sites were clustering near the 5′ half of the T loop in class I tRNAs, whereas more nucleotides in the 3′ half were involved in class II tRNAs (Kahle et al., 1990; Thurlow et al., 1991; Gaur & Krupp, 1993; Conrad et al., 1995). Similar differences were seen in the footprints, with protection at U55, C56, and G57 in pre-tRNA^{Phe} and G57, A58, and A59 in pre-tRNA^{Tyr}. Previous reports suggested that a long variable arm affected minor changes in the T loop conformation (Adlouni et al., 1993), possibly the long arm results in a tilted T loop which, moves the 3′ half more to the top of the tertiary structure, making nt 57–59 available for the interaction with RNase P. This structural difference may explain why eukaryotic RNase P cleavage is maintained after D arm deletion in the class II pre-tRNA^{Tyr} (Yuan & Altman, 1995), but abolished in the class I pre-tRNA^{Gly} (Hardt et al., 1993b). As a possible conclusion from our footprint, D arm as well as long variable arm affect a tilt in the orientation of the T loop. In deletion mutants, one of the two arms is sufficient to provide the minimal tilt required for eukaryotic RNase P cleavage. In its most reduced form, this tilt can be provided by nucleotide insertions between acceptor and T stem in minimal hairpin substrates (Carrara et al., 1995; Yuan & Altman, 1995).

Although the interpretation of our data was based on the use of a class I versus a class II tRNA, potential influences of other structural changes have to be considered also. Not only the mature tRNAs, also the lengths of both flanking sequences differ. In pre-tRNA^{Tyr}, the 3′ extension beyond the CCA sequence can stabilize the complex with M1 RNA (Hardt et al., 1995), and the long 5′ flank can affect the mode of complex formation (Guerrier-Takada & Altman, 1993). Even two different binding sites for pre-tRNA and 5′-matured tRNA have been suggested in a working model of M1 RNA (Westhof & Altman, 1994). These differences may influence the formation of initial complexes with pre-tRNA^{Tyr} and pre-tRNA^{Phe}, but the different 5′ flanks were removed by subsequent cleavage, whereas 5′-matured tRNAs were retained in the complex, in the presence of excess M1 RNA (Hardt et al., 1993a).

Based on chemical protection studies (Knap et al., 1990), it was suggested that tRNA binding to RNase P results in a partially unfolded structure at the transition between acceptor and T stem. In agreement with these conclusions, we found that complex formation resulted in exposed phosphates in this region.

As in previous studies, three general contact areas were identified: (1) next to the cleavage site at 5′ end of the acceptor stem; (2) at the 3′ CCA; and (3) in the 5′ half of the T loop with class I tRNAs (with a short variable arm) and in the 3′ half with class II tRNAs (with a long variable arm). In addition, the joint at acceptor and T stem unfolds upon RNase P RNA binding.

MATERIALS AND METHODS

RNA synthesis

M1 RNA (RNase P RNA from *E. coli*), *E. coli* pre-tRNA^{Tyr}, and *S. cerevisiae* pre-tRNA^{Phe} were prepared by in vitro transcription reactions, as described (Conrad et al., 1995). For phosphorothioate-modified RNAs, four separate transcriptions were performed in which one of the NTPs was supplemented by 5% (0.025 mM) of the desired NTPαS (obtained from Amersham or NEN). ^{32}P-end labeling was performed as described (Krupp, 1991).

Gel retardation assays

Internally labeled pre-tRNA^{Tyr} or pre-tRNA^{Phe} transcripts (10 nM) were incubated with variable amounts of M1 RNA (10–320 nM) and analyzed on 5% polyacrylamide gels as described (Hardt et al., 1993a). The fraction of complex formation was quantitated by densitometer scanning of the autoradiograms. A nonlinear least-squares equation was solved for these data, and the apparent K_d values were calculated according to the equation K_d = [active M1 RNA$_{total}$ at 50% complex] − 0.5 × [P$_{total}$], assuming that only 55% of the M1 RNA present was in an active conformation (Pyle et al., 1990; Hardt et al., 1993a).

Footprinting

In order to assure native RNA conformation, 20 ng [3′-^{32}P]-pre-tRNA (0.7 pmol; about 100 000 cpm) in 60 μL renaturation buffer (50 mM Tris-HCl, pH 8, 100 mM NH_4Cl) were kept for 3 min at 70 °C, followed by slow cooling to 37 °C, then 60 μL of 50 mM Tris-HCl, pH 8, 100 mM NH_4Cl, 200 mM $MgCl_2$ were added. The sample was split into two aliquots and the incubation was continued for 15 min in the absence or in the presence of a 50-fold molar excess of M1 RNA (about 35 pmol). Four 15-μL aliquots were taken. One aliquot served as untreated control, iodine cleavage was performed with the others by adding 1.5 μL of 1 mM, 10 mM, or 30 mM iodine in ethanol. After exactly 1 min at room temperature, reactions were stopped by ethanol precipitation, adding 1.5 μL 3 M sodium acetate, pH 5, 5 μg of glycogen, 40 μL ethanol, and freezing on dry ice. The pellet was washed with 100 μL 70% ethanol and subjected to denaturing PAGE. Scans of the resulting autoradiograms were obtained with an ULTROSCAN XL laser densitometer (Pharmacia-LKB). For each lane, the average value was determined for four slightly shifted (0.8-mm steps), nonoverlapping line tracings. The obtained band intensities were compared by superimposing the densitometer scans from reactions in the presence or absence of M1 RNA.

For sequencing reactions under denaturing conditions, the [3′-^{32}P]-tRNA was dissolved in 20 mM Hepes, pH 7, heated for 3 min at 70 °C, chilled on ice, and treated with 3 mM iodine (final concentration), as described above.

ACKNOWLEDGMENTS

D.K. received a stipend from the Konrad-Adenauer-Stiftung; R.K.G. was a fellow of the Alexander-von-Humboldt-Stiftung. This work was supported by the Deutsche Forschungsgemeinschaft (Kr 817/3-2).

Received March 27, 1996; returned for revision April 22, 1996; revised manuscript received May 17, 1996

REFERENCES

Adlouni CE, Keith G, Dirheimer G, Szarkowski JW, Przykorska A. 1993. Rye nuclease I as a tool for structural studies of tRNAs with large variable arms. *Nucleic Acids Res 21*:941–947.

Altman S, Kirsebom LA, Talbot S. 1993. Recent studies of ribonuclease P. *FASEB J 7*:7–14.

Burgin AB, Pace NR. 1990. Mapping the active site of RNase P RNA using a substrate containing a photoaffinity agent. *EMBO J 9*: 4111–4118.

Carrara G, Calandra P, Fruscolino P, Tocchini-Valentini GP. 1995. Two helices plus a linker: A small model substrate for eukaryotic RNase P. *Proc Natl Acad Sci USA 92*:2627–2631.

Conrad F, Hanne A, Gaur RK, Krupp G. 1995. Enzymatic synthesis of 2′-modified nucleic acids: Identification of important phosphate and ribose moieties in RNase P substrates. *Nucleic Acids Res 23*:1845–1853.

Eckstein F. 1985. Nucleoside phosphorothioates. *Annu Rev Biochem 54*:367–402.

Gaur RK, Krupp G. 1993. Modification interference approach to detect ribose moieties important for the optimal activity of a ribozyme. *Nucleic Acids Res 21*:21–26.

Guerrier-Takada C, Altman S. 1993. A physical assay for and kinetic analysis of the interactions between M1 RNA and tRNA precursor substrates. *Biochemistry 32*:7152–7161.

Guerrier-Takada C, Lumelsky N, Altman S. 1989. Specific interactions in RNA enzyme–substrate complexes. *Science 246*:1578–1584.

Hardt WD, Schlegl J, Erdmann VA, Hartmann RK. 1993a. Gel retardation analysis of *E. coli* M1 RNA–tRNA complexes. *Nucleic Acids Res 21*:3521–3527.

Hardt WD, Schlegl J, Erdmann VA, Hartmann RK. 1993b. Role of the D arm and the anticodon arm in tRNA recognition by eubacterial and eukaryotic RNase P enzymes. *Biochemistry 32*:13046–13053.

Hardt WD, Schlegl J, Erdmann VA, Hartmann RK. 1995. Kinetics and thermodynamics of the RNase P RNA cleavage reaction: Analysis of tRNA 3′-end variants. *J Mol Biol 247*:161–172.

Harris ME, Nolan JM, Malhotra A, Brown JW, Harvey SC, Pace NR. 1994. Use of photoaffinity crosslinking and molecular modeling to analyze the global architecture of ribonuclease P RNA. *EMBO J 13*:3953–3963.

Kahle D, Wehmeyer U, Krupp G. 1990. Substrate recognition by RNase P and by the catalytic M1 RNA: Identification of possible contact points in pre-tRNAs. *EMBO J 9*:1929–1937.

Kirsebom LA, Svärd SG. 1994. Base-pairing between *Escherichia coli* RNase P RNA and its substrate. *EMBO J 13*:4870–4876.

Kleineidam RG, Pitulle C, Sproat B, Krupp G. 1993. Efficient cleavage of pre-tRNAs by *E. coli* RNase P RNA requires the 2′-hydroxyl of the ribose at the cleavage site. *Nucleic Acids Res 21*:1097–1101.

Knap AK, Wesolowski D, Altman S. 1990. Protection from chemical modification of nucleotides in complexes of M1 RNA, the catalytic subunit of RNase P from *E. coli*, and tRNA precursors. *Biochimie 72*:779–790.

Krupp G. 1991. Direct sequence analysis of small RNAs. In: Stackebrandt E, Goodfellow M, eds. *Nucleic acid techniques in bacterial systematics*. New York: Wiley & Sons. pp 95–114.

LaGrandeur TE, Hüttenhofer A, Noller HF, Pace NR. 1994. Phylogenetic comparative chemical footprint analysis of the interaction between ribonuclease P RNA and tRNA. *EMBO J 13*:3945–3952.

Perreault JP, Altman S. 1992. Important 2′-hydroxyl groups in model substrates for M1 RNA, the catalytic RNA subunit of RNase P from *E. coli*. *J Mol Biol 226*:399–409.

Pyle AM, McSwiggen JA, Cech TR. 1990. Direct measurement of oligonucleotide substrate binding to wild-type and mutant ribozymes from *Tetrahymena*. *Proc Natl Acad Sci USA 87*:8187–8191.

Quigley GJ, Rich A. 1976. Structural domains of transfer RNA molecules. *Science 194*:796–806.

Quigley GJ, Teeter MM, Rich A. 1978. Structural analysis of spermine and magnesium ion binding to yeast phenylalanine transfer RNA. *Proc Natl Acad Sci USA 75*:64–68.

Reich C, Olsen GJ, Pace B, Pace NR. 1988. Role of the protein moiety of RNase P, a ribonucleoprotein enzyme. *Science 239*:178–181.

Rudinger J, Puglisi JD, Pütz J, Schatz D, Eckstein F, Florentz C, Giegé R. 1992. Determinant nucleotides of yeast $tRNA^{Asp}$ interact directly with aspartyl-tRNA synthetase. *Proc Natl Acad Sci USA 89*:5882–5886.

Schatz D, Leberman R, Eckstein F. 1991. Interaction of *E. coli* $tRNA^{Ser}$ with its cognate aminoacyl-tRNA synthetase as determined by footprinting with phosphorothioate-containing tRNA transcripts. *Proc Natl Acad Sci USA 88*:6132–6136.

Smith D, Burgin A, Haas ES, Pace NR. 1992. Influence of metal ions on the ribonuclease P reaction. *J Biol Chem 267*:2429–2436.

Smith D, Pace NR. 1993. Multiple magnesium ions in the ribonuclease P reaction mechanism. *Biochemistry 32*:5273–5281.

Svärd SG, Kirsebom LA. 1992. Several regions of a tRNA precursor determine the RNase P cleavage site. *J Mol Biol 227*:1019–1031.

Tallsjö A, Kirsebom LA. 1993. Product release is a rate-limiting step during cleavage by the catalytic RNA subunit of *Escherichia coli* RNase P. *Nucleic Acids Res 21*:51–57.

Thurlow DL, Shilowski D, Marsh TL. 1991. Nucleotides in precursor tRNAs that are required intact for catalysis by RNase P RNA. *Nucleic Acids Res 19*:885–891.

Westhof E, Altman S. 1994. Three-dimensional working model of M1 RNA, the catalytic RNA subunit of RNase P from *Escherichia coli*. *Proc Natl Acad Sci USA 91*:5133–5137.

Yuan Y, Altman S. 1995. Substrate recognition by human RNase P: Identification of small, model substrates for the enzyme. *EMBO J 14*:159–168.